



An experimental study on the heat dissipation of LED lighting module using metal/carbon foam[☆]

Kai-Shing Yang^a, Chi-Hung Chung^b, Ming-Tsang Lee^b, Song-Bor Chiang^a,
Cheng-Chou Wong^c, Chi-Chuan Wang^{d,*}

^a Green Energy & Environment Research Laboratories, Industrial Technology Research Institute, Hsinchu 310, Taiwan

^b National Chung Hsing University, Department of Mechanical Engineering, Taichung 402, Taiwan

^c Material & Chemical Research Laboratories, Industrial Technology Research Institute, Hsinchu 310, Taiwan

^d Department of Mechanical Engineering, National Chiao Tung University, Hsinchu 300, Taiwan

ARTICLE INFO

Available online 9 September 2013

Keywords:

LED
Metal foam
Carbon foam
Natural convection

ABSTRACT

In this study, thermal performance of the cooling modules applicable for Par 38 light bulb is investigated. A total of six heat sink modules, including the basic reference design, metal foam, and carbon foam are tested and compared. Tests are performed and analyzed using the transient test method based on JESD51-1 standard. It is found that the thermal resistance from junction to die attach is quite small. By contrast, the thermal resistance of the heat sink dominates the total resistance, and it comprises 55% of the total resistance for the standard heat sink module. With some slight opening on the base plate, the thermal resistance can be improved by approximately 12%. The thermal resistance for the carbon foam having an embedded metal plate shows the least thermal resistance of 1.14 K/W, followed by the carbon foam, and then the metal foam. The lower thermal resistance of carbon foam in association with copper metal foam is due to its higher emissivity. In addition to better heat transfer performance as compared to the standard plate heat sink, the utilization of carbon foam and metal foam can also significantly reduce the weight of the heat sink. In this study, the weight of the heat sink can be reduced as much as 33%.

© 2013 Elsevier Ltd. All rights reserved.

1. Introduction

The light-emitting diode (LED) is a semiconductor light source emitting light operated at a specific wavelength. Note that when compared to fluorescent and incandescent lighting, LEDs feature fast response time, simple structure, environmental benign, vivid colors, high energy efficiency, longevity, and easier to put into mass production. Hence, LEDs are gradually replacing traditional light sources in every aspect of lighting applications because of their versatile benefits. However, in practice LED converts only 15–30% power input into light, leaving 70–85% energy into heat. In this regard, effective thermal management of the LED lighting is imperative to avoid failure of the LEDs [1].

Thermal managements of LED lighting span three major categories: the package level, the board level, and the system level [2]. Thermal management in package level or board level involves the selection of die structure [3], die bonding material [4,5], and substrate [6]. In practice, the thermal resistance of the system level is very crucial. This is

because the size of heat sink implemented at system level normally takes up the majority of the space, weight, and surface area of the lamps and lanterns. In fact, the weight of the heat sink used in LED lighting can easily surpass 70% of its total weight. In this regard, it is crucial to reduce the size and weight of the heat sink from the standpoint of practical applications. As a consequence, cellular structure like metal foam or carbon foam can be considered as the heat sink applicable for LED lighting due to its significant reduction of weight while still retains a gigantic specific surface area for heat dissipation. There had been numerous studies associated with metal foam concerning influences like of PPI [7], and porosity [8,9] on the overall performance. Experimental and numerical studies for metal foam were also reported [10–12]. The prior study by Hsieh and Wu [13] indicated that the Nusselt number of metal foam is increased with PPI. This is because more air flow can penetrate into the internal porous structure and promote convective heat transfer. However, the rise of PPI also leads to a decline of thermal conductivity and may even deteriorate heat transfer [14].

In summary of the foregoing studies, cellular structures are considered to be very effective in heat transfer augmentation and weight reduction in natural convective applications. Hence, it is the objective of this study to investigate its applicability in typical LED applications as compared to the standard plate fin heat sink design. The cellular structures include copper metal foam and carbon foam.

[☆] Communicated by W.J. Minkowycz.

* Corresponding author.

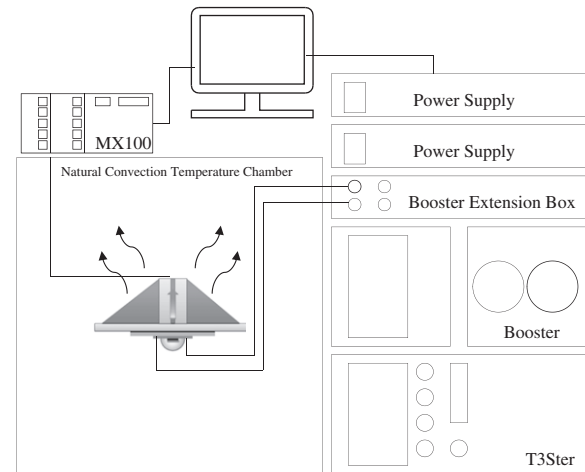
E-mail address: ccwang@mail.nctu.edu.tw (C.-C. Wang).

Nomenclature	
C [$W s K^{-1}$]	Thermal capacitance
I_F [A]	Forward current
I_H [A]	Heating current
I_M [A]	Measuring current
K [$W^2 s K^{-2}$]	Differential structure function
K_f [K/V]	K factor
k [$W m^{-1} K^{-1}$]	Thermal conductivity
t_f [mm]	Thickness of copper plate fin
t_{foam} [mm]	Thickness of copper or carbon foam
$W_{opening}$ [mm]	Width of opening
R [K/W]	Thermal resistance
T_j [$^{\circ}C$]	Junction temperature
Greek symbols	
ΔT_j	The change in the LED's junction temperature
V_f [V]	The change in the LED's forward voltage
Subscripts	
amb	Ambient
Chip	LED chip
DA	Die attach
HS	Heat sink
MCPCB	Metal Core Printed Circuit Board
th	Thermal
TP	Thermal pad
sub	substrate

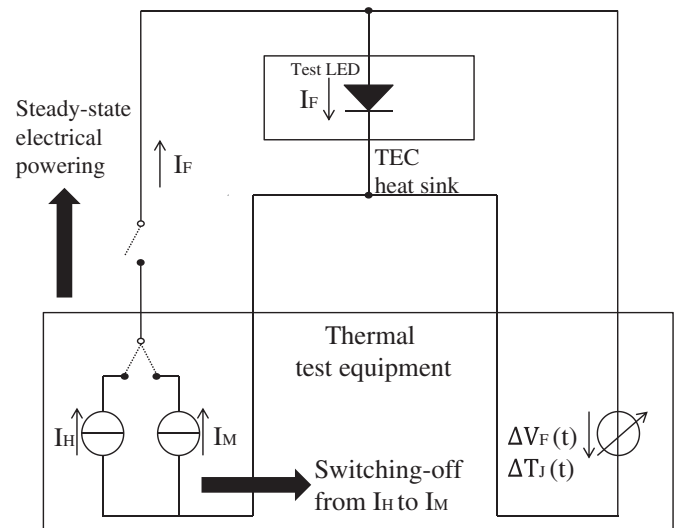
2. Experimental setup and data reduction

The schematic of the test facility is shown in Fig. 1(a) which contains an environmental chamber, a data acquisition system, a transient test measuring system (T3ster measuring system), a booster extension box, a power supply, and the test LED lighting module. The concept thermal circuit of the measurement system is depicted in Fig. 1(b). The high voltage LED lighting module is typically 1400 lm. The environmental chamber can regulate and control the ambient temperature. The ambient temperature is controlled at 25 ± 0.3 °C throughout the experiments. A total of six heat sinks are used for testing and comparing in a LED module as shown in Table 1. Detailed geometrical configurations can be seen in Fig. 2. The thickness of the base plate is 2 mm while a total of six fins having triangular configuration were mounted on the base heat sink module. The test sample #1 is the reference heat sink with a solid copper fin. Test sample #2 is identical to sample #1 except that there are some openings on the base plate. The opening is used to entrain more air from the base plate to augment heat transfer. Test sample #3 is similar to sample #1 but it replaces the copper fin with the metal foam. For sample #4, the metal foam is brazed on the copper plate. Samples #5 and #6 are similar to those of samples #3 and #4, but the metal foam is replaced by carbon foam. Both copper foam and carbon foam feature a relatively uniform distribution of pore sizes and open cell structure; the copper foam is taken from the commercially available samples and the carbon foam is made by us.

The homemade carbon foam derived from a pitch precursor because pitch is the only precursor which forms a highly aligned graphitic structure which is normally a requirement for high conductivity. The pitch was melted in 140 to 450 °C range and has risen to 400–500 °C range, causing the low molecular weight compounds in the pitch to vaporize,



(a)



(b)

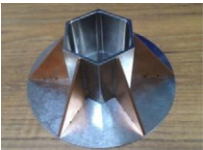
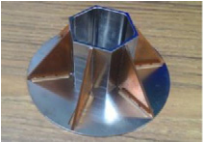

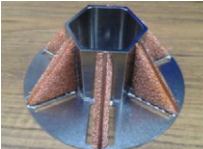


Fig. 1. Schematic of the (a) test setup (b) conceptual connection circuit for thermal circuit.

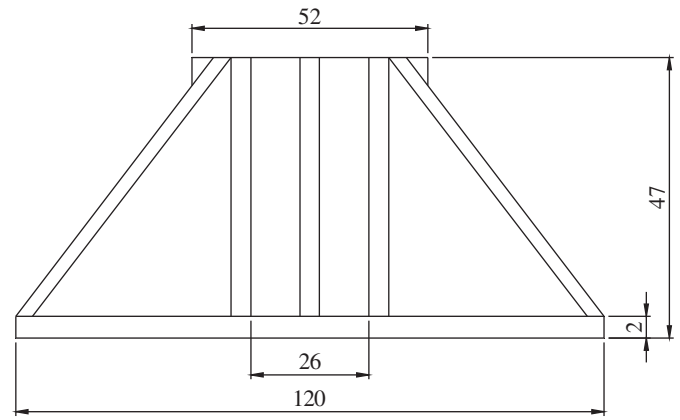
resulting in a pitch foam. Then, the pitch foam must be oxidatively stabilized by heated air. In this regard, the structure must be cross-linked and the pitch must be set so it does not melt during carbonization. The set or oxidized pitch is then carbonized in an inert atmosphere to temperatures as high as 1100 °C. Then, graphitization is performed at temperatures as high as 3000 °C to produce a high thermal conductivity graphitic structure. The thermal conductivity of a highly aligned graphitic structure in the struts was estimated to be $1700 W m^{-1} K^{-1}$. Carbon foam is a highly porosity material with k being about $150 W m^{-1} K^{-1}$, and its density is only one-fifth of the aluminum. The surface area is roughly 100 times that of the traditional heat exchanger.

The power supply into the LED module is about 9.5 W with the operational voltage and current of 267 V and 0.036 A, respectively. To minimize the thermal contact resistance, a thermal pad with $k = 2.8 W m^{-1} K^{-1}$ is used amid the LED and thermal module.

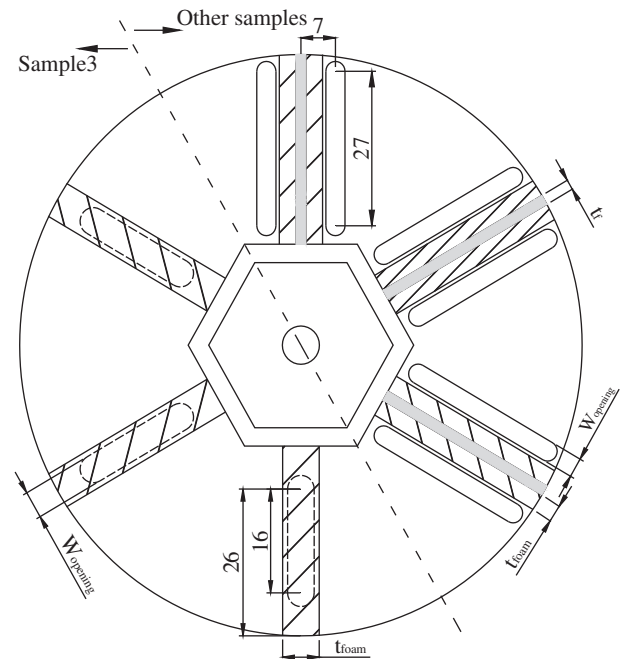
The thermal resistances of the test samples are measured using the transient test method based on EIA/JESD51-1 standard [15] (Electrical Test Method) and a transient dual interface measurement (TDIM) based on the JESD51-14standard [16]. A T3Ster Master system was used to measure the total thermal resistance of a LED based on thermal

Table 1
Photos and dimension of the heat sink modules (Unit: mm).

Sample	W_{opening}	t_f	t_{foam}	Fin type
#1 	0	1	0	Cooper plate fin
#2 	2	1	0	Copper plate fin with opening at the base
#3 	4	0	10	Cooper metal foam
#4 	2	1	4	Copper metal foam with embedded solid plate
#5 	2	0	4	Carbon foam
#6 	2	1	4	Carbon foam with embedded solid plate



(a)



(b)

Fig. 2. Detailed dimension of the heat sink module (a) side view; and (b) top view (unit: mm).

transient analysis. The measuring of T3Ster consists primarily of two parts – the hardware measurement and the software calculation. In the first step of hardware measurement, the temperature sensitivity parameter (TSP, voltage is used in this study) was measured, which is termed the K-factor. The K-factor is given as

$$K_f = \frac{\Delta T_j}{\Delta V_f} \quad (1)$$

where ΔT_j is the change in the LED's junction temperature and ΔV_f is the change in the LED's forward voltage. To calibrate the K-factor, 1 mA bias current was used from ambient temperature of 25 °C to 85 °C as shown in Fig. 3. The device under test was located in the chamber with the forward voltage of the LED diode which was measured at different temperatures. Notice that the relation of the forward-voltage drop of a junction and the temperature of that junction is nearly linear, therefore the K-factor is obtained. Hence, the calibrated K-factor is 5.97 K/V.

In the second step of the hardware measurement, the forward-voltage transient data were recorded to determine the junction temperature change with the fixed ambient temperature. The applied current pulse and voltage vary during the measurement of thermal resistance. A bias current was first applied initially for certain period, and then the current level was quickly switched to a higher level and stayed there till the steady state of the LED was reached. Later on, the driving current was replaced with the bias current, and the voltage transient data were recorded subject to natural convective cooling process. In this experiment, bias current was 1 mA and the operational current is 36 mA. The cooling curve was transformed into a Foster R-C network, which is called network identification by deconvolution. The differential structure function is defined as the derivative of the cumulative thermal capacitance with respect to the thermal resistance. The differential structure function represents the thermal resistance from the junction to the ambient.

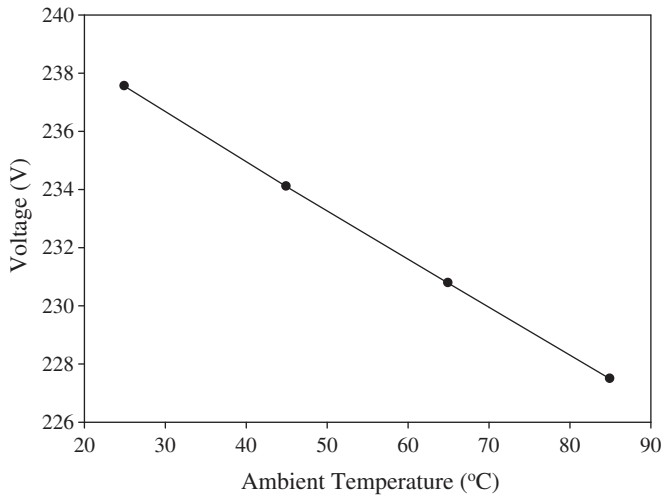


Fig. 3. Calibration of K-factor against ambient temperature.

3. Results and discussion

As can be seen in the thermal resistance structure in Fig. 4, the resistance path for the LED package consists of a chip (designated as A), a die attach (B), a substrate (C), a MCPCB (D), a thermal pad (E), and the heat sink module (F). Tests are conducted with the same LED module subject to six different heat sinks at the fixed ambient temperature of 25 °C. The structure function of the reference sample (#1) is shown in Fig. 5. It is interesting to note that the heat sink module represents the major thermal resistance of 55%, while the percentages of the thermal resistance to the total thermal resistance of the die, die attach, substrate, MCPCB, and thermal pad are, 3%, 3%, 12%, 19%, and 8%, respectively. The results implicate that the thermal resistance subject to natural convection on the heat sink is the detrimental one. On the other hand, the thermal resistance of die and die attach is almost negligible. The results are opposite to the numerical simulations carried out by Christensen and Graham [17]. In their study, they clearly showed that the major thermal resistance in the die and die attach comprises more than 65% of the total thermal resistance. The results are quite confusing at first sight. However, the difference can be made clear from the study of Ji and Moon [18] who clearly showed that the thermal resistance of the die attach is strongly related to the die attach materials themselves. For example, at a same thickness of 30 μm , the thermal resistance is 32 °C/W for Ag epoxy while it is appreciably reduced to 2.9 °C/W for the PbSn Solder. In this study, the die attached materials are also of PbSn solder type, thereby showing a rather small thermal resistance from the junction to the die attached.

The test results for all the heat sink modules are displayed in Fig. 6. Note that the test samples use the same LED/package/substrate. As a consequence, the basic structure function for all the test samples shows a nearly identical structure in regions A–D. The major difference in the structure function occurs mainly on the heat sink. However, thermal pad is used as a link between the LED package and the heat sink. The adhesion of LED package and heat sink using thermal pad depends on human operation. This is because some micro air gap may exist in the thermal pad adhesion subject to human operation, and resulting in some slight differences in thermal resistance of the thermal pad. In this regard, one can see that there are some minor departures of the structure function in the thermal pad region (E region). To overcome this situation, a transient dual interface measurement (TDIM) based on the EIA/JESD51-14 standard [16] is conducted to minimize the human error. The process is made available by adding a low thermal conductivity material on the thermal pad, causing an increased thermal resistance of the thermal

pad. Hence, the rise of the effective thermal resistance in the E region will reduce the error of the thermal pad.

The structure functions of all samples are shown in Fig. 7. From Fig. 7, the corresponding thermal resistance of thermal pad and heat sink can be obtained, and it is shown in Fig. 8. It is found that the sample with carbon foam having an embedded metal plate (sample #6) shows the least thermal resistance of 1.14 K/W, followed by samples #5, #2, #4, #3 and #1. However, the pure carbon foam (sample #5) shows an almost identical thermal resistance of 1.16 K/W as compared to that of sample #6. Notice that the reference heat sink with solid copper fin shows the largest thermal resistance of 1.47 K/W. On the other hand, the fin for sample #2 is identical to that of sample #1 but it has several extra openings in the base plate. Hence, the design will entrain airflow from the base and lead to an appreciable drop of thermal resistance to 1.29 K/W. In addition to the benefits of improvement in thermal resistance, the utilization of carbon foam can also significantly reduce the weight of the heat sink. In this study, the weight of the heat sink can be reduced by as much as 33% as shown in Fig. 8.

With the pure metal foam (sample #3), the thermal resistance is reduced by 10% to 1.31 K/W. The improvements by metal foam are in line with the measurements of Xu et al. [19] who conducted natural convection for air in horizontally-positioned open-celled metal foams. Their results showed that the thermal resistance was reduced in the order of 10% as compared to that of solid metal. Although the specific surface area of metal foam is tremendously increased, the rise of surface area does not proportionally contribute to enhance heat transfer. This is associated with several reasons. Firstly, with the high porosity of the metal foam, its thermal conductivity is significantly reduced. For instance, Sadeghi et al. [20] reported that the effective thermal conductivity of aluminum metal foam is in the order of 3.78–7.37 W/m which is nearly one to two orders lower than that of the pure aluminum. In this regard, conduction contribution in the metal foam is appreciably reduced and fin efficiency of the metal foam is also considerably decreased. However, the significant decline in thermal conductivity may not be the detrimental reason. This can be made clear from sample #4 which is also made from metal foam but it is embedded with a solid copper plate amid the metal foam. It appears that the thermal resistance is only moderately reduced to 1.24 K/W. However, its corresponding effective thermal conductivity is increased at least 20 times. Test results of Xu et al. [20] for various porosities and PPI metal foams also show only moderate difference in natural convective thermal resistance (around 5–15%). Secondly, the porous structure of metal foam provides significant viscous force for the air flow within the metal foam, limiting the air flow movement and convection accordingly. Hence, the thermal resistance for metal foam is only slightly reduced in response to these

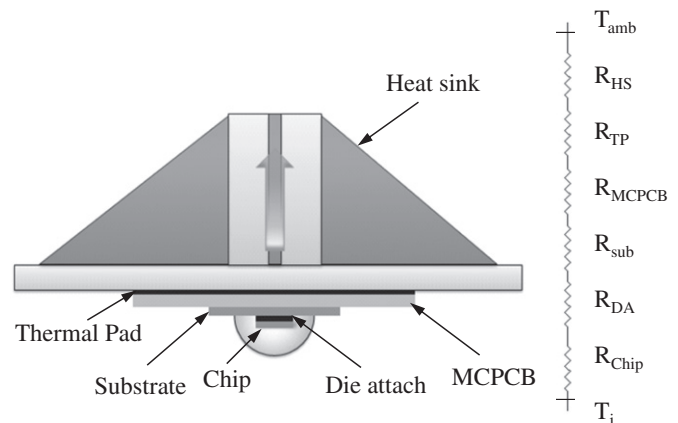
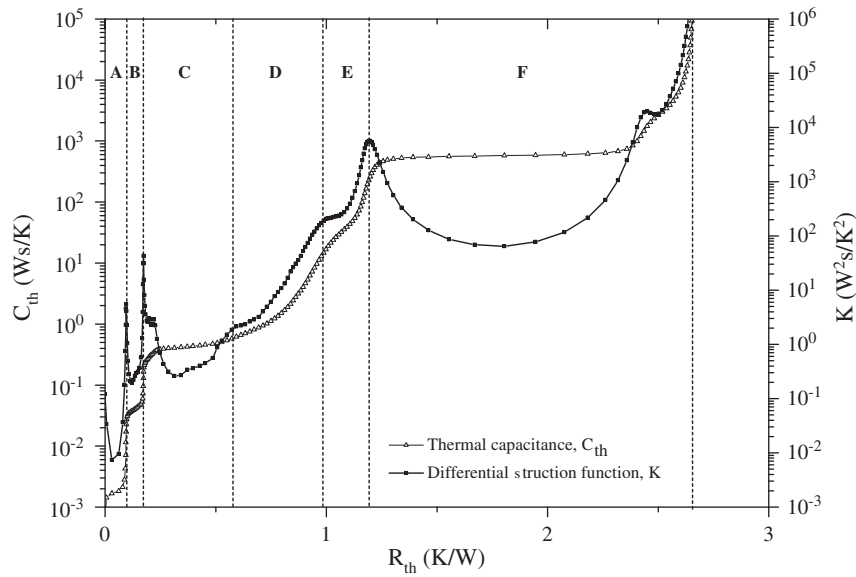
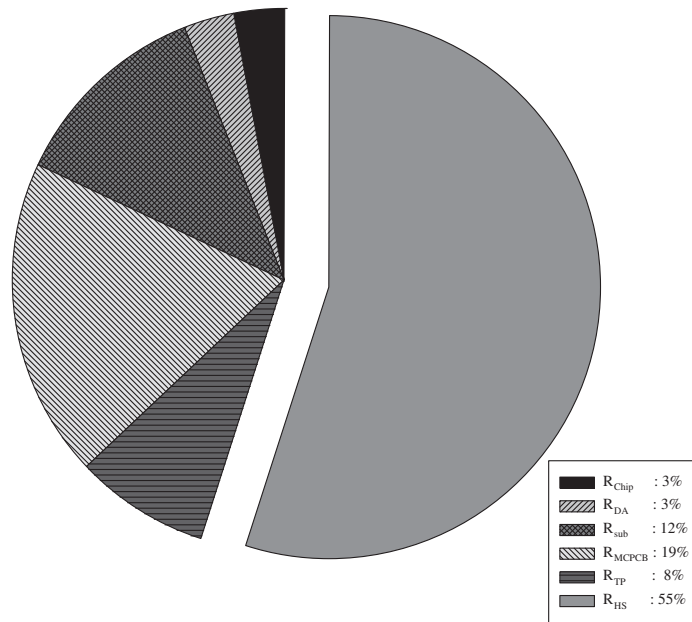


Fig. 4. Schematic of the thermal network for a LED light bulb.



(a)



(b)

Fig. 5. (a) Structure function for sample #1 and (b) thermal resistance percentage along the thermal pass.

two effects. The test results show that the carbon foam shows the smallest thermal resistance of 1.14 K/W. The marginal decrease in thermal resistance for carbon foam may be mainly associated with its higher emissivity (around 0.69, using Emissivity Measure model from Japan Sensor Corporation, model TSS-5X) which is much higher than that of the metal foam (~ 0.03), therefore the carbon foam shows a marginally lower thermal resistance.

4. Conclusions

In this study, an experimental study is conducted in cooling of LED using metal/carbon foam. A total of six heat sink modules are made and are implemented on a typical PAR38 LED light bulb. The test sample #1 is the reference heat sink with a solid copper fin. Test sample #2 is

identical to sample #1 except that there are some openings on the base plate. Test sample #3 is similar to sample #1 but it replaces the copper fin with the metal foam. For sample #4, the metal foam is brazed on the copper plate. Samples #5 and #6 are similar to samples #3 and #4 but the metal foam is replaced by carbon foam. The tests are performed using the transient test method based on JESD51-1 standard. Test results for the six samples are concluded as follows:

- (1) The thermal resistance from junction to die attach is quite small. This is associated with the die-attached material.
- (2) It is found that the thermal resistance of the heat sink is the dominant one which accounts for 55% of the total resistance for the standard heat sink module. With some slight opening on the base plate, the thermal resistance can be improved by approximately 12.2%.

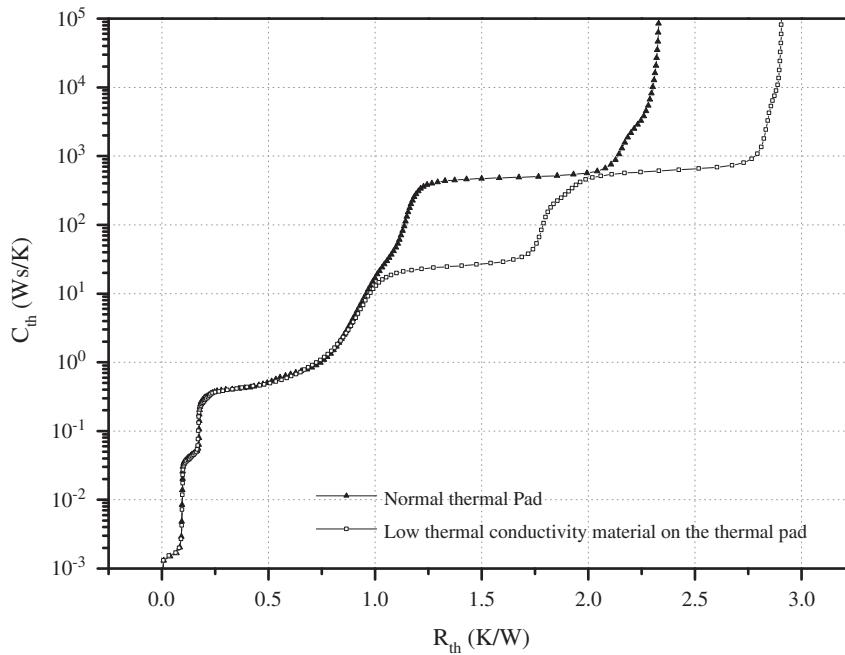


Fig. 6. Structure function for LED modules with various thermal pads.

- (3) The thermal resistance for the carbon foam having an embedded metal plate shows the least thermal resistance, followed by carbon foam, and metal foam. The lower thermal resistance of carbon foam is due to its higher emissivity which gives rise to larger radiation contribution. In addition to the benefits of improvement in thermal resistance, the utilization of carbon foam can also significantly reduce the weight of the heat sink. In this study, the weight of the heat sink can be reduced as much as 33%.
- (4) The thermal resistance of the metal foam is about 15.6% lower than that of the standard heat sink module. The thermal resistance of

the metal foam is about 3.8% lower than that of the standard heat sink module with opening at the base.

Acknowledgments

This work has been supported by the Energy Bureau from the Ministry of Economic Affairs. Also grant from National Science Committee of Taiwan is appreciated.

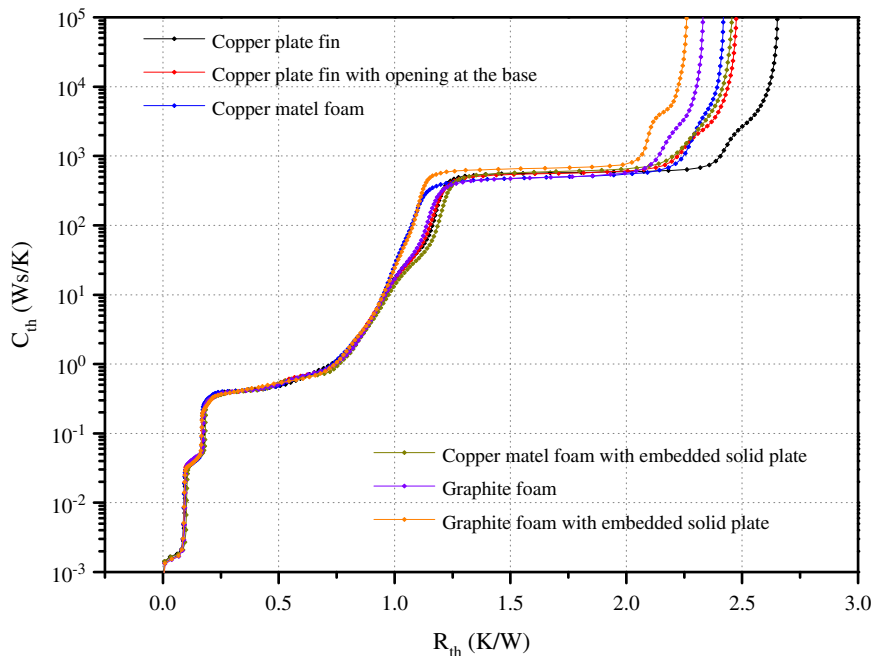


Fig. 7. Structure function for various LED modules.

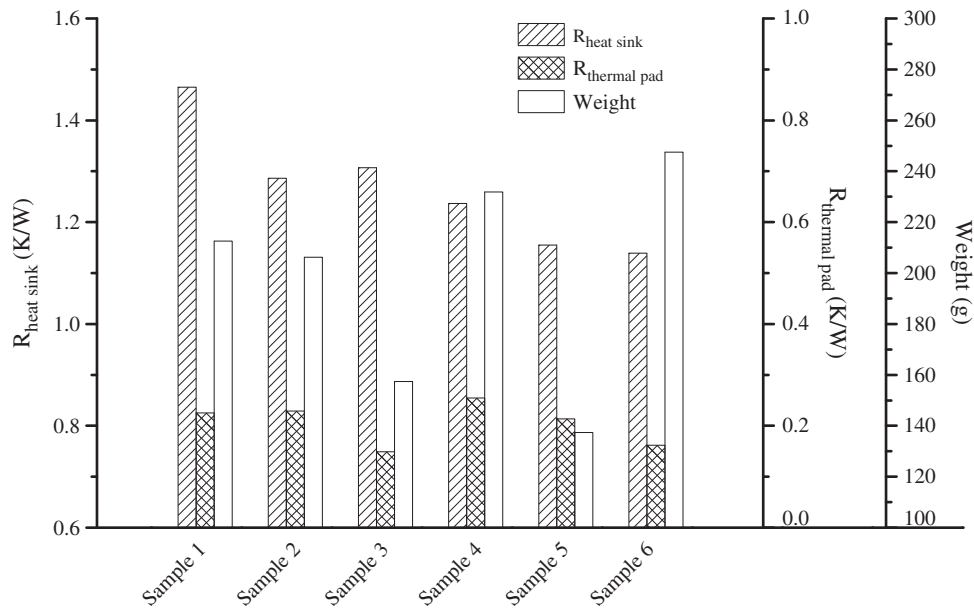


Fig. 8. The thermal resistance and weight of the LED modules.

References

- [1] N. Narendran, Y. Gu, J.P. Freyssinier, H. Yu, L. Deng, Solid-state lighting: failure analysis of white LEDs, *J. Cryst. Growth* 268 (2004) 449–456.
- [2] H.H. Wu, K.H. Lin, S.T. Lin, A study on the heat dissipation of high power multi-chip COB LEDs, *J. Microelectron.* 49 (2012) 280–287.
- [3] C.A. Tran, C.F. Chu, C.C. Cheng, W.H. Liu, J.Y. Chu, H.C. Cheng, F.H. Fan, J.K. Yen, T. Doan, High brightness GaN vertical light emitting diodes on metal alloyed substrate for general lighting application, *J. Cryst. Growth* 298 (2007) 722–724.
- [4] R.H. Horng, J.S. Hong, Y.L. Tsai, D.S. Wu, C.M. Chen, C.J. Chen, Optimized thermal management from a chip to a heat sink for high-power GaN-based light-emitting diodes, *IEEE Trans. Electron Devices* 57 (2010) 2203–2207.
- [5] B.H. Liou, C.M. Chen, R.H. Horng, Y.C. Chiang, D.S. Wu, Improvement of thermal management of high-power GaN-based light-emitting diodes, *Microelectron. Reliab.* 52 (2012) 861–865.
- [6] L. Yin, L. Yang, W. Yang, Y. Guo, K. Ma, S. Li, J. Zhang, Thermal design and analysis of multi-chip LED module with ceramic substrate, *Solid-State Electron.* 54 (2010) 1520–1524.
- [7] A. Bhattacharya, R.L. Mahajan, Metal foam and finned metal foam heat sinks for electronics cooling in buoyancy-induced convection, *J. Electron. Packag.* 128 (2006) 259–266.
- [8] M.S. Phanikumar, R.L. Mahajan, Non-Darcy natural convection in high porosity metal foam, *Int. J. Heat Mass Transf.* 45 (2002) 3781–3793.
- [9] S. Mancin, C. Zilio, A. Cavallini, L. Rossetto, Heat transfer during air flow in aluminum foams, *Int. J. Heat Mass Transf.* 53 (2010) 4976–4984.
- [10] G. Hetsroni, M. Gurevich, R. Ozenblit, Natural convection in metal foam strips with internal heat generation, *Exp. Therm. Fluid Sci.* 32 (2008) 1740–1747.
- [11] G. Hetsroni, M. Gurevich, R. Ozenblit, Sintered porous medium heat sink for cooling of high-power mini-devices, *Int. J. Heat Fluid Flow* 27 (2006) 259–266.
- [12] C.Y. Zhao, T.J. Lu, H.P. Hodson, Natural convection in metal foams with open cells, *Int. J. Heat Mass Transf.* 48 (2005) 2452–2463.
- [13] W.H. Hsieh, J.Y. Wu, Experimental investigation of heat-transfer characteristics of aluminum-foam heat sinks, *Int. J. Heat Mass Transf.* 47 (2004) 5149–5157.
- [14] Z. Qu, T. Wang, Experimental study of air natural convection on metallic foam-sintered plate, *Int. J. Heat Mass Transf.* 38 (2012) 126–132.
- [15] EIA/JESD51-1 standard, Integrated circuits thermal measurement method—electrical test method (single semiconductor device), Electronic Industries Association, 1995.
- [16] JESD51-14 standard, Transient dual interface test method for the measurement of the thermal resistance junction to case of semiconductor devices with heat flow through a single path, 2010.
- [17] A. Christensen, S. Graham, Thermal effects in packaging high power light emitting diode arrays, *Appl. Therm. Eng.* 29 (2009) 364–371.
- [18] P.F. Ji, C.H. Moon, Effects of some factors on the thermal-dissipation characteristics of high-power LED packages, *J. Inf. Disp.* 13 (2012) 1–6.
- [19] Z.G. Xu, Z.G. Qu, C.Y. Zhao, Experimental study of natural convection in horizontally-positioned open-celled metal foams, 20–22 May 2011 2011 International Conference on Materials for Renewable Energy & Environment (ICMREE), 1, Institute of Electrical and Electronics Engineers, Shanghai, China, 2011, pp. 923–928.
- [20] E. Sadeghi, S. Hsieh, M. Bahrami, Thermal conductivity and contact resistance of metal foams, *J. Phys. D: Appl. Phys.* 44 (2011) 125406.